GC&times&GC measurements of C7?C11 aromatic and n-alkane hydrocarbons on Crete, in air from Eastern Europe during the MINOS campaign

X. Xu, J. Williams, C. Plass-Dülmer, H. Berresheim, G. Salisbury, L. Lange, J. Lelieveld

Atmos. Chem. Phys. Discuss., 3, 1477–1513, 2003
www.atmos-chem-phys.org/acpd/3/1477/

Atmospheric Chemistry and Physics Discussions

GC×GC measurements of C_7 – C_{11} aromatic and n-alkane hydrocarbons on Crete, in air from Eastern Europe during the MINOS campaign

X. Xu[1], J. Williams[1], C. Plass-Dülmer[2], H. Berresheim[2], G. Salisbury[1], L. Lange[1], and J. Lelieveld[1]

[1]Max Planck Institute for Chemistry, Mainz, Germany
[2]German Weather Service, Meteorological Observatory Hohenpeissenberg, Germany

Received: 23 January 2003 – Accepted: 11 March 2003 – Published: 17 March 2003

Correspondence to: X. Xu (xu@mpch-mainz.mpg.de)

Abstract

During the Mediterranean Intensive Oxidant Study (MINOS) campaign in August 2001 gas-phase organic compounds were measured using comprehensive two-dimensional gas chromatography (GC×GC) at the Finokalia ground station, Crete. In this paper, $C_7 - C_{11}$ aromatic and n-alkane measurements are presented and interpreted. The mean mixing ratios of the hydrocarbons varied from 1±1 pptv (i-propylbenzene) to 43±36 pptv (toluene). The observed mixing ratios showed strong day-to-day variations and generally higher levels during the first half of the campaign. Mean diel profiles showed maxima at local midnight and late morning, and minima in the early morning and evening. Results from analysis using a simplified box model suggest that both the chemical sink (i.e. reaction with OH) and the variability of source strengths were the causes of the observed variations in hydrocarbon mixing ratios. The logarithms of hydrocarbon concentrations were negatively correlated with the OH concentrations integral over a day prior to the hydrocarbon measurements. Slopes of the regression lines derived from these correlations for different compounds are compared with literature rate constants for their reactions with OH. The slopes for most compounds agree reasonably well with the literature rate constants. A sequential reaction model has been applied to the interpretation of the relationship between ethylbenzene and two of its potential products, i.e. acetophenone and benzeneacetaldehyde. The model can explain the good correlation observed between [acetophenone]/[ethylbenzene] and [benzeneacetaldehyde]/[ethylbenzene]. The model results and field measurements suggest that the reactivity of benzeneacetaldehyde may lie between those of acetophenone and ethylbenzene and that the ratio between yields of acetophenone and benzeneacetaldehyde may be up to 28:1. Photochemical ages of trace gases sampled at Finokalia during the campaign are estimated using the sequential reaction model and related data. They lie in the range of about 0.5-2.5 days.

ACPD

3, 1477–1513, 2003

1. Introduction

Atmospheric volatile organic compounds (VOCs) are recognized as important atmospheric species affecting air chemistry on regional and global scales. Photochemical reactions of hydrocarbons in the atmosphere lead to the formation of ozone, oxygenates and organic aerosols (Fehsenfeld et al., 1992; Andreae and Crutzen, 1997; Limbeck and Puxbaum, 1999; Krivácsy et al., 2001; O'Dowd et al., 2002).

Atmospheric VOCs are released by various anthropogenic and biogenic sources. The use of fossil fuels, especially oil, is the largest anthropogenic VOC source, while emission from vegetation, mainly in the form of isoprene and monoterpenes, is the dominant source of biogenic VOCs (Fuentes et al., 2000; Guenther et al., 2000; IPCC, 2001). Biomass burning, caused by natural and human activities, also releases significant amounts of VOCs into the atmosphere (Andreae and Merlet, 2001).

Increased use of gasoline and other hydrocarbon products has caused enhanced emissions of non-methane hydrocarbons (NMHCs), especially alkanes and alkyl-substituted aromatics (IPCC, 2001). This not only lowers the air quality of source regions, but also alters air composition and quality of remote regions through long-distance transport of NMHCs and their photochemical degradation products, as seen in the Mediterranean region (Lelieveld et al., 2002). Because of their direct reactions with OH and the subsequent formation of ozone, NMHCs can influence the distribution and budget of tropospheric OH, as shown by model studies (Houweling et al., 1998; Wang et al., 1998). Since atmospheric properties and climate are closely related to aerosol concentrations, levels of ozone and other greenhouse gases, enhanced NMHC emissions may potentially influence climate.

The large number of components directly emitted by various sources and formed during photochemical reactions make air samples very complex. The complexity adds difficulties to the measurements of individual or groups of atmospheric components. Special measures, such as chromatographic separation, are needed to avoid interferences from non-targeted components. In some cases, such as laboratory and in-

ACPD
3, 1477–1513, 2003

situ photochemical studies, simultaneous measurements of a large number of components are highly desirable. A common method for simultaneous measurements of many VOCs is to use capillary gas chromatography (GC), in combination with a flame ionization detector (FID) or a mass spectrometer (MS) (e.g. Helmig et al., 1996; Rappenglück et al., 1998; Wedel et al., 1998). However, conventional GC, being limited by the separation power of single column, often fails to separate components in complex samples to a satisfactory degree. As recently shown by Lewis et al. (2000) and Xu et al. (2003), even ambient air samples are complex enough, so that severe overlap may occur in the conventional GC measurements, resulting in erroneous identification and quantification of components.

We have applied a new technique, the comprehensive two-dimensional gas chromatography (GCxGC), to the in-situ measurement of atmospheric VOCs. In this paper we present data of $C_7 - C_{11}$ aromatic and n-alkane hydrocarbons measured at a remote Mediterranean site, discuss their variations, and interpret them using data from other observations, especially the OH concentration. The instrumentation, as well as the identification and quantification techniques, are described in a separate paper (Xu et al., 2003).

2. Experimental

2.1. Site

The in-situ measurements described here were performed during the Mediterranean Intensive Oxidant Study (MINOS) campaign in August 2001 (summarized by Lelieveld et al. (2002)). Atmospheric VOCs were observed at Finokalia, Crete, a ground-based station (35°19' N, 25°40' E; 130 m asl) established by the University of Crete. Crete is located roughly in the middle of the Eastern Mediterranean, about 400 to 1000 km away from the coasts of Greece and Turkey. The wind was steady and northerly throughout the campaign. The windspeed averaged 7.4 $m\,s^{-1}$, corresponding to a transport time

of 0.5-1.5 days from continental coastal sources to the measurement point.

The Finokalia station is located at the top of a hill facing the sea within the 270°–90° sector (Mihalopoulos et al., 1997). During the MINOS campaign, the GC×GC system was installed in one of the three instrument containers, placed on the seaward side of the hill, about 50 m west of and 20 m below the station, in a bend of an unasphalted road. The horizontal distance between the containers and the sea was approximately 200 m. Only a few vehicles per day passed the upwind section of the road. Due to the influence of coastal orography the wind direction observed at the site was south-westerly to northwesterly, showing diel features. This local wind system does not lead to significant influence of emissions from other parts of Crete on the measurements (Mihalopoulos et al., 1997). On the upwind side of the container there were some small shrubs (< 1 m) covering about 50% of the ground. Peaks of biogenic species scarcely showed up on the chromatograms of ambient air samples, suggesting that emissions from the local vegetation had no significant influence on the observed VOC concentrations for most of the time during the campaign.

2.2. Sampling and measurement of VOCs

An on-line sampling and measurement system was used for the in-situ observation of atmospheric VOCs. The system consists of a flow controller and a thermal desorber (both from Markes International, Pontyclun, UK), and a gas chromatograph (GC6890, Agilent, Wilmington, DE, USA), equipped with an FID and jet-modulated GC×GC parts (Zoex, Lincoln, NE, USA). Details about the whole system are given in Xu et al. (2003).

Ambient air from a height of about 7 m above the ground was drawn continuously through a main sample line (Teflon, 10 m, 9 mm I.D.) at about 100 l min^{-1} by a high volume pump. A sub-stream (50 ml min^{-1}) of air was drawn through a Teflon manifold connected to the main sample line, a Teflon tube (1 m, 3.18 mm O.D.), and the link tube (stainless steel, 89 mm, 6.35 mm O.D.) and cold trap (quartz, 12 mm, 2 mm I.D.) of the thermal desorber by a membrane pump, to trap VOCs in the sampled air (3–4 l). The cold trap contains two beds of sorbent, i.e. Tenax TA and Carbograph, supported

by quartz wool. During the sampling the sorbent beds of the cold trap were cooled by a 2-stage peltier cell to enhance the focusing efficiency. For the measurements on a few days, a Nafion dryer (Markes International, Pontyclun, UK) was used to remove water vapor from the air samples. In this case, the sorbent beds of the cold trap were cooled to -10°C. A disadvantage of using Nafion dryers is that they can remove some polar organic compounds such as some oxygenated hydrocarbons. To avoid loss of oxygenated hydrocarbons, the Nafion dryer was bypassed for most of the time during the campaign. A focusing temperature of 10°C was then used, instead of -10°C. These changes, however, should not have any effects on the hydrocarbon data presented in this paper.

For the GC×GC measurements, a long DB-5 column (30 m, 0.25 mm I.D., 1 μm (5%-phenyl)-methylpolysiloxane film) and a short Carbowax column (1 m, 0.1 mm I.D., 0.1 μm polyethylene glycol film) were used as the first and second columns, respectively. A modulation period of 6 seconds was applied to obtain two-dimensional chromatograms. This has proven suitable for air samples, which usually contain components of very different polarities. Helium (99.9999%, Messer Griesheim, Frankfurt, Germany) was used as carrier and purge gas. It was further purified using water vapor, hydrocarbon, and oxygen filters (Sigma-Aldrich, Deisenhofen, Germany) included in the carrier gas line. For the separation, the first column was heated at a rate of 2.5°C min^{-1} from 50°C to 200°C, and the second column at a rate of 2.5°C min^{-1} from 30°C to 180°C. With an analysis time of 60 min compounds between C_7 and C_{14} were well separated. Compounds more volatile than n-heptane were not or less satisfactorily resolved. Since these lighter compounds were measured during MINOS using the GC-MS and PTR-MS techniques (see Gros et al., 2003; Salisbury et al., 2003), the GC×GC system was optimized for measuring heavier compounds.

To determine the blank, helium samples (2–3 l) were collected and analyzed using the same system and method as for the air measurements. The blank measurements were made once every 2–3 days. Blank levels for some compounds were relatively high during the first half of the campaign. After the cold trap and a filter (6 mm, PTFE)

in the flow-path of the thermal desorber were changed on 12 August 2001, blank concentrations decreased to significantly lower levels and remained low until the end of the campaign.

The system was calibrated approximately once every 5 days by measuring a standard gas mixture containing 74 hydrocarbons in nitrogen (Apel-Riemer Environmental, Denver, USA). Only two point calibrations were made, so as not to detract from the measurement frequency of air samples. Laboratory multipoint calibrations showed a very good linear dependence of peak sizes (i.e. volumes of 2D peaks) on the injected component masses. Standards for oxygenated hydrocarbons were not available. Acetophenone and benzeneacetaldehyde measurements, which are used in this paper (Section 3.5), have been calibrated using standard measurements of ethylbenzene and a FID response factor of 0.8 (Katritzky et al., 1994). Based on the field measurements of the standard, the (1σ) precisions for the quantified hydrocarbons are estimated to be 5–28%. The errors of the standard concentrations are 2%, as given by the manufacturer. Taking into account errors in the volume determination and the peak integration, the accuracy for the hydrocarbons is estimated to be about 5%. Due to the indirect calibrations of acetophenone and benzeneacetaldehyde, the accuracy for these species may be worse. A realistic estimate of the accuracy may be 15%, including a 10% error in the response factor. For the acetophenone and benzeneacetaldehyde measurements from the periods 2–4 August and 7–10 August, there may be additional errors due to potential influences of the Nafion dryer on these two oxygenates. 1,2,4-trimethylbenzene was subject to a significant interference by octanal; consequently, the measurements of this species are not shown, even though it might have significantly contributed to the total aromatic hydrocarbon. Depending on components, the (2σ) detection limit was between 0.2 and 35 pptv in the first half of the campaign and between 0.2 and 12 pptv in the second half of the campaign. More details about the instrumentation, and the identification and quantification of the various compounds are given in Xu et al. (2003)

3. Results and discussion

3.1. Overview

Measurements of atmospheric VOCs covered the period of 2–21 August 2001. The time resolution of the measurements was about 2 h, including one hour analysis and one hour cooling of column ovens. System purging and sampling overlapped the measurement time for the previous sample, hence needed no extra time. Although uninterrupted measurement was intended, there were some measurement gaps due to instrument malfunctions and delays in liquid nitrogen supply. Statistical results of all hydrocarbon measurements are listed in Table 1. For the purpose of comparison, Table 1 also shows some data from the hydrocarbon measurements from the Greater Athens Area (GAA) of Greece (Rappenglück et al., 1998). Since the GAA is one of the nearest polluted areas upstream of Crete, a comparison of hydrocarbon measurements from Finokalia with those from the GAA may give a measure of the remoteness of the Finokalia site, though the measurements were not made in the same time period. From the mean values, Table 1 shows that the mixing ratios for the n-alkanes at Finokalia are about one order of magnitude lower than those in the GAA. The differences between the two sites are even larger for the aromatic hydrocarbons. The mixing ratios of most aromatic hydrocarbons at Finokalia are approximately two orders of magnitude lower than those in the GAA. The large differences suggest that Finokalia is a site far from anthropogenic sources.

Under the assumptions that the mean concentration profile obtained at Finokalia was a photochemically aged concentration profile of the GAA air and that the background levels were negligible for all the components, it appears that a large discrepancy existed between n-alkanes and aromatics (excluding o-xylene and 1,3,5-trimethylbenzene), with the n-alkane levels at Finokalia corresponding to much smaller (a factor of 2–3) photochemical ages than the aromatic levels. The mean concentrations of o-xylene and 1,3,5-trimethylbenzene seem to be relatively too high and inconsistent with those of the other aromatics. These discrepancies may be attributed to the assumptions

ACPD
3, 1477–1513, 2003

that are not necessarily valid, i.e. the concentration profile of the GAA air was not representative and the background levels were not negligible for some components (e.g. n-alkanes). Another reason for the discrepancies could be unknown systematic errors in the data, caused by analytical problems (e.g. peak overlaps or calibration errors).

Even though Finokalia is a remote site, the influences of anthropogenic hydrocarbons on the local atmospheric chemistry are not negligible in terms of the OH budget. If only the primary reaction with OH is considered, the summed, average reactivity (defined by $\Sigma k_i[X_i]$, with k_i being the rate constant for the reaction of X_i with OH) caused by NMHCs listed in Table 1 is equivalent to 18% of that caused by CH_4 (at 1.8 ppmv), which is one of the major contributors to the OH budget. This is a lower limit estimate of the anthropogenic influence, as this does not include the intermediate products, nor the compounds outside the C_7–C_{11} scale of the measurements.

The anthropogenic influences were highly variable during the campaign, as can be seen in Fig. 1, which shows the summed mixing ratios of C_8-C_{11} n-alkanes and C_7-C_{10} aromatics during the MINOS campaign. The general trends of the two quantities as well as the individual species were similar during the campaign, showing higher levels at the beginning and in the middle and lower levels in the last week of the campaign. The variations of the hydrocarbon levels were caused by changes of air masses and the strength of the chemical sink, i.e. the removal by reaction with OH.

Although the observed wind directions at the Finokalia site during the campaign were southwesterly to northwesterly, with a clear diurnal oscillation between southwest and northwest, backward air trajectories show that air masses were transported to Finokalia from the northwest to northeast sector (Salisbury et al., 2003). Based on the air trajectories and the measurements of important trace gases, such as CO, CH_3CN, and Rn, Salisbury et al. (2003) divided the whole campaign into 4 periods, with some transitions. Time intervals corresponding to periods 2–4 are indicated in Fig. 1 by the vertical dashed lines. No GC×GC measurement is available for period 1.

Since most of the hydrocarbons under consideration are very reactive, with lifetimes

ACPD
3, 1477–1513, 2003

of a few hours, the air mass history during the 1–2 days prior to the arrival time is relevant to the abundances of the hydrocarbons. In the transition between periods 1 and 2, air masses arriving at Finokalia were two days previously over the Black Sea and transported over western Turkey and the Aegean Sea. Hydrocarbon data from these days can be characterized by strong diurnal variations and a significant decreasing trend. Air masses arriving at Finokalia during period 2 were from higher altitudes (> 2 km) over the North Sea and travelled eastwards to the Black Sea and then southwestwards through the boundary layer to Finokalia (Salisbury et al., 2003). Limited measurements from this period do not show significant influence of the descending air masses on the measured concentrations of the reactive hydrocarbons, although such influence is visible in the propane data, which show lower values during period 2 than during the rest of the campaign (Gros et al., 2003). This is not surprising because the air masses might have been polluted 1–2 days prior to their arrival as they entered the continental boundary layer. In period 3, air over Finokalia was strongly influenced by biomass burning emissions, as indicated by the high mixing ratio of acetonitrile, a marker of biomass burning. In this period, the mixing ratios of hydrocarbons showed very strong fluctuations and some high values. Due to technical problems with the cold trap, GC×GC measurements were not reliable for the period between 10 August, 21:00 UTC and 12 August, 21:00 UTC, where strongest biomass burning signatures were observed (Salisbury et al., 2003). This measurement gap, together with the strong fluctuations, make it difficult to identify components that were significantly influenced by biomass burning emissions. Some significant increases in the nighttime concentrations during period 3 probably imply biomass burning emissions of octane, nonane, toluene, ethylbenzene, xylenes, trimethylbenzenes, methylethylbenzenes, and diethylbenzenes. However, this is very uncertain, especially for toluene, trimethylbenzenes, and methylethylbenzenes, which showed some high concentrations also in the transition prior to periods 2. Although biomass burning influence still can be seen in periods 4, as indicated by some spikes in the acetonitrile measurements (Salisbury et al., 2003), GC×GC measurements from this period show significantly lower hydrocarbon levels than those from

other periods, with the exception of the beginning and end. As will be discussed later, the lower hydrocarbon levels were at least partly caused by the higher OH abundance in the second half of the campaign.

3.2. Diel variation

As already mentioned, the mixing ratios of hydrocarbons showed significant diel variations, especially when the mixing ratios were high. To see the general features of the diel variation, mixing ratios from the individual measurements were normalized to corresponding daily means from the days on which the measurements were made, and the normalized mixing ratios from different days were averaged to obtain mean diel profiles for the whole campaign. Figure 2 shows the mean diel profiles for some n-alkane and aromatic hydrocarbons observed during the campaign. Although there are slight differences between the profiles for different compounds, the general features are consistent. Hydrocarbon levels were relatively high at local midnight and decreased towards the early morning. After 6:00 local time, they increased rapidly, peaked at about 10:00, and then decreased slowly until about 20:00. There are several factors that may cause diel variations of hydrocarbon mixing ratios, with source variability and reaction with OH being the most important two for the hydrocarbons under consideration. These two factors will be discussed in the following sections.

3.3. Variability of sources and chemical sinks

The fluctuations of hydrocarbon source strengths are of interest, because they can be directly related to the emission activities. At sites near sources, source variations dominate the variations of hydrocarbon mixing ratios. Therefore, observed fluctuations of mixing ratios are very similar to those of the source strength. At the remote sites, however, the similarity between both types of fluctuation is usually bad, due to the influences of dilution and chemical reactions on the mixing ratios. This is especially true for the reactive hydrocarbons, such as those listed in Table 1. Simultaneous measure-

ments of hydrocarbons and OH, however, make it possible to obtain information about the relative variability of the hydrocarbon sources and chemical sinks. This section presents an approach using a simplified box model.

Atmospheric abundance of any gas is controlled by the sources and sinks of the gas. Changes in the sources and sinks result in a temporal variation in the abundance of the gas. The temporal variation in the abundance of hydrocarbon X in a well mixed box can be described as

$$\frac{d[\mathrm{X}]}{dt} = S - k[\mathrm{OH}][\mathrm{X}], \quad (1)$$

where [X] and [OH] are the mixing ratios of X and OH, respectively; t is time; k is the rate constant for the reaction of X with OH; S is the net physical source/sink of X, including contributions from emissions, transport and dilution. Note that the reactions of X with oxidants other than OH (e.g. O_3, NO_3, etc.) are not considered in this simplified box model, because for the hydrocarbons in consideration, these reactions are at least one order of magnitude slower than the reaction with OH under the campaign conditions. The model also neglects deposition, which is probably of minor importance for the NMHCs considered.

For most of the campaign, OH was measured at 5 min time resolution (Berresheim et al., 2003) and hydrocarbons were measured about every 2 h. Simultaneous measurements of hydrocarbons and OH facilitate the calculation of the instantaneous variation of [X] (i.e. d[X]/dt) and the chemical sink (i.e. k[OH][X]). Based on the box model shown in Eq. (1), the term (S) can be readily calculated as

$$S = \frac{d[\mathrm{X}]}{dt} + k[\mathrm{OH}][\mathrm{X}]. \quad (2)$$

Since S also contains contributions of transport and dilution, the value of S can be negative due to influx of cleaner air masses into the box.

Before the calculation using Eq. (2) could be carried out, some interpolations and extrapolations in the hydrocarbon and OH data were necessary. For the periods 6–8

ACPD
3, 1477–1513, 2003

August, 9–11 August, and 13–18 August 2001, the measured OH can be well described by the empirical function [OH] = $aJ_{O(^1D)}^{0.68}$, with a = 1.5 × 10^{10} cm^{-3}, 1.8 × 10^{10} cm^{-3}, and 2.4 × 10^{10} cm^{-3}, respectively (Berresheim et al., 2003). This empirical function was used for interpolating OH data for the measurement gaps in the period 6–18 August. Since no OH measurement is available for the first a few days of the campaign, an extrapolation was done to obtain OH data for the period 2–6 August. Because it is not known which of the three a values is the best for this period, the average of them was used for the extrapolation. Hydrocarbon measurements were interpolated using the cubic spline method to obtain time series with one point per hour. For large measurement gaps (> 8 h), the interpolated data may contain features that are not real; data points associated with these gaps were therefore deleted from the final results. The interpolated time series were differentiated to obtain d[X]/dt.

Figure 3 shows the variations in the calculated S and chemical sink (k[OH][X]) of ethylbenzene during the period 13–19 August 2001. The loss of ethylbenzene due to the reaction with OH followed the typical diel profile of OH, showing a peak around midday Crete time (ca. 10:00 UTC) and values close to zero during the night. The value of S had a major peak around the local noon, coinciding with the peak of the chemical sink. The combination of the variations in the source and sink terms resulted in daytime concentration peaks (around 10:00 local time, see Fig. 2). In comparison with the chemical sink, S showed more features. Besides the major peak, it had one or more peaks of medium or small size during the night. Since the nocturnal reaction of hydrocarbon with OH was negligible, any change in the term S resulted immediately in a change in the concentration of the hydrocarbon. Therefore, nighttime peaks in S were responsible for the high midnight values in the diel profiles shown in Fig. 2.

Reasons for the strong variation of S and its patterns shown in Fig. 3 are not very clear. Although unstable local emissions could explain the observed variation of S, it is believed that influences of emissions from Crete are not significant in the summer months (Mihalopoulos et al., 1997). The estimated trace gas ages were all higher than 10 h, suggesting that contributions of local emissions were of minor importance (see

Sect. 3.5 and Salisbury et al., 2003). Therefore, it seems unlikely that the variation of S was caused by local sources. Since S, by definition, also includes the contribution of transport, transport of air masses with varying hydrocarbon concentrations have probably been responsible for the observed variation of S. Consequently, the hydrocarbon concentrations were probably less influenced by the level of local OH, but more by the average level of OH along the back trajectories, which showed that air masses travelled about 0.5–1 days from the coast of the mainland to Finokalia (Salisbury et al., 2003).

3.4. Hydrocarbon-OH relationship

Since the reaction with OH is one of the key factors driving the concentration variations of reactive hydrocarbons, one can expect certain hydrocarbon-OH relationships. The relationship cannot easily be revealed by simply comparing individual hydrocarbon measurements with the corresponding average OH concentrations because the hydrocarbon levels at any time depend on the previous source and sink strengths. OH concentration integrated over a certain period prior to the hydrocarbon measurement (i.e. $\int_{-T}^{0}[\mathrm{OH}]dt$) may be a suitable quantity for a comparison with hydrocarbon measurements. Data from the MINOS campaign support this idea. Figure 4 shows a negative correlation between ln[Decane] and $\sum[\mathrm{OH}]t$, with the later being the integral of OH over a 24-h period before the hydrocarbon measurement (i.e. $\sum[\mathrm{OH}]t \equiv \int_{-24}^{0}[\mathrm{OH}]dt$). This negative correlation suggests that lower hydrocarbon levels are related to higher previous OH levels (higher $\sum[\mathrm{OH}]t$). Similar correlations like that shown in Fig. 4 (i.e. $ln[\mathrm{X}] = a - b\sum[\mathrm{OH}]t$) were also observed for the other hydrocarbons, with most of the correlations being significant at the confidence level of 99%.

The $ln[\mathrm{X}] - \sum[\mathrm{OH}]t$ correlations may be explained using the simplified box model, i.e. Eq. (1). The analytical solution of Eq. (1) for the time interval [0,t] is

$$ln[\mathrm{X}] = ln([\mathrm{X}]_0 + \int_0^t Se^{k\int_0^t[\mathrm{OH}]dt}dt) - k\int_0^t[\mathrm{OH}]dt, \quad (3)$$

with $[\mathrm{X}]_0$ being the initial concentration of X. In laboratory experiments, S can be set

to zero and [OH] can be held constant, so that the variation of hydrocarbon X can be described by $ln[X] = ln[X]_0 - k[OH]t$. In the atmosphere, the situation is more complicated, since both S and [OH] can vary considerably. Because a nonzero S makes a disturbance ($\int_0^t S e^{k\int_0^t [OH]dt} dt$) to the measured $ln[X]$ as well as a varying $[X]_0$, a perfect $ln[X]$-$\int_0^t [OH]dt$ correlation seldom exists in the atmosphere. Depending on the intensity of the disturbance, a more or less degraded correlation or poor correlation can be observed. The $ln[X] - \sum[OH]t$ correlations observed during the MINOS campaign (e.g. Fig. 4) are probably such degraded correlations. Although they are statistically significant, their correlation coefficients (0.30–0.72) indicate that the OH reaction accounts only for 9–52% of the variance of $ln[X]$, depending on components. The remainder should be due to the disturbance from S.

The disturbances from S and $[X]_0$ may also affect the intercept and slope of the correlation line. If the disturbances are of minor importance, the slope of the observed $ln[X] - \sum[OH]t$ correlation line can be treated as an estimated rate constant (k) for the reaction of X with OH, obtained from an experiment under real atmospheric conditions. During the MINOS campaign, however, S varied significantly (see Fig. 3), so that the slopes might have strongly deviated from the k values. Nevertheless, it is of interest to compare the slopes for different components with the corresponding k values. In Fig. 5 the slopes for components for which significant $ln[X] - \sum[OH]t$ correlations were observed are plotted against the corresponding k values from the literature (Atkinson, 1986; Atkinson and Aschmann, 1989; Nolting et al., 1988; Ohta and Ohyama, 1985). For most components the slopes agree with the literature k values within a factor of two. For the two trimethylbenzenes the slopes are about 3-4 times lower than the k values. The disagreement between the slopes and the k values can be attributed to uncertainties caused by using the highly simplified box model and by neglecting S and the $[X]_0$ variation in the empirical approach and to errors in the slopes and k values. For some components, e.g. the trimethylbenzenes, large disagreements may indicate large systematic errors in the measurements (see Sect. 3.1).

Use of the OH concentration integrated over a 24-h period is not physically required,

ACPD
3, 1477–1513, 2003

but empirically selected. Considering the short (a few hours) lifetimes of the hydrocarbons, a smaller timescale seems more suitable for the integration. However, the $ln[X] - \sum[OH]t$ correlations become much less significant if OH is integrated over smaller timescales. Actual reasons for this phenomenon are unknown. One of the reasons might be that the OH level along the air trajectories was important for the observed hydrocarbon concentrations and the 24-h period best represented the average time that air masses needed to travel from the source regions to Finokalia (see discussions in the previous section).

3.5. Sequential reaction model and photochemical age

In this work hydrocarbons and their degradation products were simultaneously measured using the same GC×GC system. Consequently, the in-situ GC×GC measurements can be used for studying photochemical processing and testing reaction mechanisms. This section shows an application of a sequential reaction model to the measurements of ethylbenzene and its products (see Fig. 6).

The sequential reaction model was proposed by Bertman et al. (1995) and has been successfully used for interpretation of ambient measurements of alkanes and alkyl/peroxyacetyl nitrates (Bertman et al., 1995; Roberts et al., 1998, 2001), and of isoprene and its products, i.e. methacrolein and methylvinyl ketone (Stroud et al., 2001). The model describes the time dependence of the [product]/[precursor] ratio in a reaction sequence like

$$A \xrightarrow{k_a} B \xrightarrow{k_b} C, \tag{4}$$

where k_a and k_b are the rate constants for the reactions of an oxidant (e.g. OH) with A and B, respectively. For a chamber study with zero initial concentration of B, the model predicts

$$\frac{[B]}{[A]} = \frac{k_a}{k_b - k_a}\left(1 - e^{(k_a - k_b)t}\right), \tag{5}$$

ACPD
3, 1477–1513, 2003

where [A] and [B] are the concentrations of A and B at time t, respectively.

The application of the model to ambient data requires a number of assumptions, including (1) emission of the precursor by a point source or an ensemble of similar sources, (2) negligible contribution of other chemical/physical sources to the product, (3) negligible background levels of the precursor and product, (4) removal of the product only through photochemical processes, and (5) constant kinetic parameters over the period of reaction (Bertman et al., 1995; Roberts et al., 2001). In the atmosphere it is often difficult to fulfill all the assumed conditions. However, large deviations from the assumptions may be revealed by comparing observed and predicted data, if all kinetic data are available. In some cases, substantial differences between the observed and predicted data can provide evidence of unknown processes (see e.g. Bertman et al., 1995; Roberts et al., 1998, 2001).

Atmospheric ethylbenzene is mainly removed by OH-initiated reactions. Although the rate constant for the ethylbenzene + OH reaction has been well determined, little is known about the detailed mechanism of ethylbenzene degradation. It is believed that pathways of the ethylbenzene + OH reaction include OH addition to the aromatic ring and OH abstraction of an H-atom from the ethyl group, with the former leading to formation of ethylnitrophenols, furandiones, etc., and the latter leading to formation of acetophenone, benzeneacetaldehyde, and benzaldehyde (Hoshino et al., 1978; Forstner et al., 1997). Note that both pathways require the presence of O_2 and NO_x. Neglecting the rapid intermediate reactions, the degradation of ethylbenzene via acetophenone and benzeneacetaldehyde can be simplified as

$$\mathrm{EB} \xrightarrow{\alpha k_1} \mathrm{AP} \xrightarrow{k_2} \mathrm{products}, \quad (6)$$

$$\mathrm{EB} \xrightarrow{\beta k_1} \mathrm{BA} \xrightarrow{k_3} \mathrm{products}, \quad (7)$$

where EB, AP, and BA denote ethylbenzene, acetophenone, and benzeneacetaldehyde, respectively; k_1, k_2, and k_3 are the rate constants for the reactions of OH with ethylbenzene, acetophenone, and benzeneacetaldehyde, respectively; and α and β are the respective yields of acetophenone and benzeneacetaldehyde. Although both

ACPD
3, 1477–1513, 2003

acetophenone and benzeneacetyldehyde may also be formed from other precursors (see e.g. Bignozzi et al., 1981), ethylbenzene is probably the predominant chemical source due to its high abundance. If contributions of other precursors are neglected, the variations of the mixing ratios of ethylbenzene ([EB]), acetophenone ([AP]), and benzeneacetaldehyde ([BA]) can be described by

$$\frac{d[\mathrm{EB}]}{dt} = -k_1[\mathrm{OH}][\mathrm{EB}], \tag{8}$$

$$\frac{d[\mathrm{AP}]}{dt} = \alpha k_1[\mathrm{OH}][\mathrm{EB}] - k_2[\mathrm{OH}][\mathrm{AP}], \tag{9}$$

$$\frac{d[\mathrm{BA}]}{dt} = \beta k_1[\mathrm{OH}][\mathrm{EB}] - k_3[\mathrm{OH}][\mathrm{BA}]. \tag{10}$$

Assuming that [OH] takes its average value for the campaign, analytical solutions for Eqs. (8)–(10) can be obtained. From the solutions the following expressions can be derived

$$\frac{[\mathrm{AP}]}{[\mathrm{EB}]} = \frac{\alpha k_\mathrm{A}}{k_\mathrm{B} - k_\mathrm{A}}\left(1 - e^{(k_\mathrm{A}-k_\mathrm{B})t}\right) + \frac{[\mathrm{AP}]_0}{[\mathrm{EB}]_0}e^{(k_\mathrm{A}-k_\mathrm{B})t}, \tag{11}$$

$$\frac{[\mathrm{BA}]}{[\mathrm{EB}]} = \frac{\beta k_\mathrm{A}}{k_\mathrm{C} - k_\mathrm{A}}\left(1 - e^{(k_\mathrm{A}-k_\mathrm{C})t}\right) + \frac{[\mathrm{BA}]_0}{[\mathrm{EB}]_0}e^{(k_\mathrm{A}-k_\mathrm{C})t}, \tag{12}$$

where $k_\mathrm{A} = k_1[\mathrm{OH}]$, $k_\mathrm{B} = k_2[\mathrm{OH}]$, and $k_\mathrm{C} = k_3[\mathrm{OH}]$. Assuming that the initial ratios of both products to ethylbenzene are close to zero, the second term on the right-hand side of Eqs. (11) and (12) can be neglected. In this case, the [product]/[precursor] ratios are dependent only on time, and the following relationship can be derived from the modified Eqs. (11) and (12)

$$\frac{[\mathrm{AP}]}{[\mathrm{EB}]} \approx \frac{\alpha}{\beta} \cdot \frac{k_\mathrm{C} - k_\mathrm{A}}{k_\mathrm{B} - k_\mathrm{A}} \cdot \frac{1 - e^{(k_\mathrm{A}-k_\mathrm{B})t}}{1 - e^{(k_\mathrm{A}-k_\mathrm{C})t}} \cdot \frac{[\mathrm{BA}]}{[\mathrm{EB}]}. \tag{13}$$

To see the actual relationship between [AP]/[EB] and [BA]/[EB], the ratios have been calculated from the in-situ measurements of ethylbenzene, acetophenone, and benzeneacetaldehyde (Fig. 6). The ratios that were derived from the measurements above the detection limits are plotted against each other in Fig. 7. It appears that the two ratios are linearly correlated within their ranges found at Finokalia. A least-square fit gives a regression line with a negligible intercept (0.4). The correlation is significant, as indicated by the correlation coefficient (0.80).

It should be emphasized that some other factors may cause similar correlation as that in Fig. 7. For example, one may obtain correlations by comparing concentration ratios between any two of three reactive components that are primarily emitted by common sources. In this case, the correlations may be caused by dilution and parallel photochemical decay of different components (see e.g. Roberts et al., 1984; Rudolph and Johnen, 1990; McKeen and Liu, 1993). Parallel decay and dilution should lead to similar trends in the concentrations of all components. However, data in Fig. 6 show that the concentrations of acetophenone and benzeneacetaldehyde seem to be anti-correlated with that of ethylbenzene, inconsistent with the consequence of parallel decay and dilution. In the present study and in Stroud et al. (2001), two ratios that are partially dependent on each other are compared. This is a substantial change to the original applications (Bertman et al., 1995; Roberts et al., 1998, 2001), which used independent ratios. A drawback of such change is that the correlation between the ratios cannot completely be attributed to sequential reactions, because the variation in the common denominator of the two ratios can cause an "artificial" correlation, especially if the variations of the numerators (e.g. concentrations of long-lived gases) are much smaller than that of the denominator (e.g. a reactive gas). Consequently, it should be avoided to correlate two [product]/[precursor] ratios with each other, if the reactivity of the products is much lower than that of the precursor. In the present study, differences in the OH rate constant between the products and precursor are less than a factor of 3 (see the discussions later) and the variabilities of the products are comparable to that of the precursor; therefore, it is likely that the observed correlation shown in Fig. 7 is

mainly a result of sequential reactions.

It would be interesting to compare the empirical result shown in Fig. 7 with the theoretical result from Eq. (13). Unfortunately, a direct comparison is impossible in the present study because both β and k_C in Eq. (13) are unknown. Nevertheless, some postulations can be made on the basis of the data shown here.

Since the observed lowest [BA]/[EB] and [AP]/[EB] (close to 0.1 and 2, respectively) are very small in comparison with most of the measured values, the assumption of zero initial [product]/[precursor] ratios seems to be valid for the data set shown in Fig. 7. Although both acetophenone and benzeneacetaldehyde are produced and used in perfumery, flavor, and pharmaceutical industries, the fossil fuel emissions of ethylbenzene are probably the predominant source, so that the initial ratios at the source regions may be neglected.

Rate constants at 298 K for the reactions of OH with ethylbenzene and acetophenone are 7×10^{-12} and 2.7×10^{-12} cm^3 $molecule^{-1}$ s^{-1}, respectively (Kwok and Atkinson, 1995; Calvert et al., 2002). The slower reaction of acetophenone with OH leads to an increase of [AP]/[EB] with reaction time. Reports of the rate constant for the benzeneacetaldehyde + OH reaction are currently lacking. Figure 7 shows that about one fifth of the observed [BA]/[EB] ratios are larger than unity, implying that benzeneacetaldehyde is less reactive than ethylbenzene. On the other hand, it is likely that benzeneacetaldehyde reacts with OH more rapidly than acetophenone does, because of the higher reactivity of the -CHO group. Therefore, benzeneacetaldehyde is probably more reactive than acetophenone and less reactive than ethylbenzene. In other words, the rate constant for the benzeneacetaldehyde + OH reaction is likely to be in the range of $2.7\text{-}7 \times 10^{-12}$ cm^3 $molecule^{-1}$ s^{-1}. Assuming that the rate constants for the reactions of OH with acetophenone and benzeneacetaldehyde are close to each other, Eq. (13) can be approximated to $\frac{[AP]}{[EB]} \approx \frac{\alpha}{\beta} \cdot \frac{[BA]}{[EB]}$. This postulated linear relationship between the ratios is consistent with the linear correlation shown in Fig. 7. Comparing this approximate expression with the empirical equation given in Fig. 7, and neglecting the small intercept observed empirically, an α/β ratio of 28 may be obtained, suggesting that

the yield for acetophenone may be 28 times as high as that of benzeneacetaldehyde. However, this value should be considered as an upper limit, because the reactivity of benzeneacetaldehyde may be higher than that of acetophenone, as mentioned above, so that a slope of 28 could still exist with a lower α/β value (see Eq. (13)).

To the best of our knowledge, there has been no report of the yield of benzeneacetaldehyde from the ethylbenzene + OH reaction. Measurements in the gas phase and in secondary organic aerosol (SOA) did not show benzeneacetaldehyde as a product from photooxidation of ethylbenzene (Hoshino et al., 1978; Forstner et al., 1997). Theoretically, this compound could be formed via the abstraction of a β-hydrogen atom from the ethyl group. Hoshino et al. (1978) excluded the possibility of this mechanism because they did not find a detectable amount of benzeneacetaldehyde. However, it seems likely that this compound is produced at a very low yield, so that it is not easily observed. Based on the data of Hoshino et al. (1978), the yield of acetophenone is close to 0.5. If 28 is a realistic value for α/β, the corresponding β value should be about 0.02. Complete separation of analytes and high sensitivity of detection system are necessary to detect products with such a low yield.

Sequential reaction models can be used to derive information about the photochemical evolution of trace gases, expressed as "photochemical age", from the field measurements of a precursor and its product. If the initial concentration of the product is negligible, only kinetic data and observed [product]/[precursor] ratios are needed, while in the alternative method using the [tracer]/[tracer] ratio, the initial ratio between tracers of interest is necessary (see e.g. Roberts et al., 1984; Rudolph and Johnen, 1990; Salisbury et al., 2003). Photochemical ages of trace gases encountered at Finokalia during MINOS were calculated from the observed [acetophenone]/[ethylbenzene] ratios using Eq. (11). The initial [acetophenone]/[ethylbenzene] ratio was assumed to be zero. The yield of acetophenone (α) is assumed to be 0.5, based on the laboratory data of Hoshino et al. (1978). An average OH abundance of 4.5×10^6 cm^{-3} (Berresheim et al., 2003) was used and assumed to be applicable to all transport ways of the air masses. The calculated photochemical ages, coded in color in Fig. 7, lie in the range of 15-59

h, with an average of about 37 h. Since the age calculation includes only data points with ethylbenzene above the detection limit, the average photochemical age may be slightly underestimated. The estimated trace gas ages suggest that pollutants had experienced 15–59 h of reaction before arriving at Finokalia, corresponding to transport distances of ∼ 400–1600 km at an average windspeed of 7.4 m s^{-1}. These limits are approximately the distances from Finokalia to the coasts of Greece and Turkey and to the East European countries, including Bulgaria, Romania, and Ukraine, respectively.

Salisbury et al. (2003) estimated the trace gas ages for the same site and time periods 1–3 using average [toluene]/[benzene] ratios. The estimated average ages were 34 h and 15 h for periods 2 and 3, respectively. Average ages from the present study are 25±6 h for period 2 and 22±4 h for period 3. Although the different sampling rates used for the PTR-MS and GC×GC measurements and gaps in GC×GC measurements may have effects on the estimated average photochemical ages, the estimated ages from both methods agree reasonably well.

The results from the sequential reaction model should be treated with caution although they seem sound. There may be large uncertainties caused by correlating two [product]/[precursor] ratios that are partially dependent on each other, by applying assumptions that may be invalid, and by neglecting some important factors. Correlating two partially interdependent [product]/[precursor] ratios seems not to significantly change the relationship between the ratios, as implied by the data in a previous study (Stroud et al., 2001). However, it cannot be tested presently whether or not the fitted slope (28) in Fig. 7 is close to the theoretical value, due to the lack of some kinetic data. Neglecting backgrounds of the precursor and products may be problematic. While the background may be insignificant for ethylbenzene and benzeneacetaldehyde, it is probably not negligible for acetophenone, which showed concentrations of 20–200 pptv. Another problem may be applying the sequential reaction model to data from a remote site that is hundreds to thousands km distant to continental sources. Such large distances increase the possibility of collecting air affected by very different sources, which may cause additional errors in the results.

4. Conclusions

Atmospheric VOCs at Finokalia, Crete, were measured during MINOS using the novel GC×GC technique. The observed mean mixing ratios of $C_7 - C_{11}$ aromatics and n-alkanes were 1–2 orders of magnitude lower than those observed at a suburban site of Athens, suggesting that Finokalia is far from the sources, being predominantly anthropogenic. In spite of the remoteness of Finokalia, influences of anthropogenic hydrocarbons on the photochemistry at the site are not negligible in terms of the OH reaction. Even if only the primary reaction with OH is considered, the summed, average reactivity caused by the hydrocarbons considered in this paper is 18% of that caused by CH_4. Since heavier hydrocarbons, especially aromatics, produce a lot of reaction intermediates that contribute to O_3 chemistry and that may be precursors of organic aerosols, the role of long-range transport of these hydrocarbons to remote regions warrants further study.

Mixing ratios of the hydrocarbons were in the pptv to sub-ppbv range, showing significant day-to-day and diurnal variations. These variations were caused partially by changes in the OH abundance, but to a larger extent by varying hydrocarbon sources, as shown by the analysis using a simplified box model. Comparing $/n$[X] with $\sum$[OH]t makes clear the influence of OH concentration on the hydrocarbon concentrations, which is hardly visible if instantaneous [X] and [OH] are compared. Another advantage of such comparison is that it allows derivation of correlation line slopes, which are equivalent to the rate constants for the X + OH reactions, estimated under atmospheric conditions. In spite of the varying source strengths, the slopes for most components agree with the literature k values within a factor of two.

The strong separation power of the GC×GC technique makes the simultaneous measurement of many VOCs more reliable. There is a great need for reliable field measurements of atmospheric hydrocarbons and their degradation products for use in studies of photochemical processing, such as testing reaction mechanisms and validating model results. As an example, the present paper shows the application of a

ACPD
3, 1477–1513, 2003

sequential reaction model to the interpretation of the observed relationship between [acetophenone]/[ethylbenzene] and [benzeneacetaldehye]/[ethylbenzene]. Acetophenone and benzeneacetaldehyde are two of the potential products of the ethylbenzene + OH reaction. Although theoretical mechanisms indicate the possibility of benzeneacetaldehyde as a product, this compound has not been detected as a product of the ethylbenzene photooxidation in laboratory studies. Based on results from this study, it is likely that benzeneacetaldehyde is produced in the reaction, albeit in rather small yield. The rate constant for the benzeneacetaldehyde + OH reaction has not presently been reported. Data from the present study suggest that the rate constant may lie in the range of $2.7–7.0\times10^{-12}$ $cm^3\,molecule^{-1}\,s^{-1}$. Photochemical ages of trace gases sampled at Finokalia have been estimated using the sequential reaction model and related data. They lie in the range of 0.5–2.5 days, supporting the idea that pollutants were mainly transported from East European countries to the East Mediterranean during MINOS.

Acknowledgements. We are grateful to M. de Reus for her excellent coordination of the MINOS campaign. We thank N. Mihalopoulos and his colleagues, and the local coordinator P. Petsalakis for their logistical support. J. Beens, L. van Stee, and M. Adahchour contributed to the identification of the 2D peaks. Technical support from F. Helleis, M. Flanz, G. Schebeske, T. Klüpfel, and D. Scharffe were important for the preparation and implementation of the measurements.

References

Andreae, M. O. and Crutzen, P. J., Atmospheric aerosols: Biogeochemical sources and role in atmospheric chemistry, Science, 276, 1052–1058, 1997. 1479

Andreae, M. O. and Merlet, P.: Emission of trace gases and aerosols from biomass burning, Global Biogeochem. Cycles, 15, 955–966, 2001. 1479

Atkinson, R.: Kinetics and mechanisms of the gas-phase reactions of the hydroxyl radical with organic compounds under atmospheric conditions, Chem. Rev., 86, 69–201, 1986. 1491, 1506

Atkinson, R. and Aschmann, S. M.: Rate constants for the gas-phase reactions of the OH radical with a series of aromatic hydrocarbons at 296 ± 2 K, Int. J. Chem. Kinet., 21, 355–365, 1989. 1491, 1506

Berresheim, H., Plass-Dülmer, C., Elste, T., Mihalopoulos, N., and Rohrer, F.: OH in the coastal boundary layer of Crete during MINOS: Measurements and relationship with ozone photolysis, Atmos. Chem. Phys. Discuss., 3, 1183-1212, 2003. 1488, 1489, 1497, 1506

Bertman, S. B., Roberts, J. M., Parrish, D. D., Buhr, M. P., Goldan, P. D., Kuster, W. C., Fehsenfeld, F. C., Montzka, S. A., and Westberg, H.: Evolution of alkyl nitrates with air mass age, J. Geophys. Res., 100, 22 805–22 813, 1995. 1492, 1493, 1495

Bignozzi, C. A., Maldotti, A., Chiorboli, C., Bartocci, C., and Carassiti, V.: Kinetics and mechanism of reactions between aromatic olefins and hydroxyl radicals, J. Chem. Kinet., 13, 1235–1242, 1981. 1494

Calvert, J. G., Atkinson, R., Becker, K. H., Kamens, R. M., Seinfeld, J. H., Wallington, T. J., and Yarwood, G.: The mechanisms of atmospheric oxidation of aromatic hydrocarbons, Oxford University Press, New York, 2002. 1496

Fehsenfeld, F., Calvert, J., Fall, R., Goldan, P., Guenther, A. B., Hewitt, C. N., Lamb, B., Liu, S., Trainer, M., Westberg, H., and Zimmerman, P.: Emissions of volatile organic compounds from vegetation and implications for atmospheric chemistry, Global Biogeochem., 6(4), 389–430, 1992. 1479

Forstner, H. J. L., Flagan, R. C., and Seinfeld, J. H.: Secondary organic aerosol from the photooxidation of aromatic hydrocarbons: Molecular composition, Environ. Sci. Technol., 31, 1345–1358, 1997. 1493, 1497

Fuentes, J. D., Lerdau, M., Atkinson, R., Baldocchi, D., Bottenheim, J. W., Ciccioli, P., Lamb, B., Geron, C., Gu, L., Guenther, A., Sharkey, T. D., and Stockwell, W.: Biogenic hydrocarbons in the atmospheric boundary layer: A review, Bull. Amer. Meterol. Soc., 81, 1537–1575, 2000. 1479

Gros, V., Williams, J., van Aardenne, J., Salisbury, G., Hofmann, R., Lawrence, M., von Kuhlmann, R., Lelieveld, J., Krol, M., Berresheim, H., Lobert, J. M., and Atlas, E.: Origin of anthropogenic hydrocarbons and halocarbons measured in the summertime European outflow (on crete 2001), submitted to Atmos. Chem. Phys., 2003. 1482, 1486

Guenther, A., Geron, C., Piece, T., Lamb, B., Harley, P., and Fall, R.: Natural emissions of nonmethane volatile organic compounds, carbon monoxide, and oxides of nitrogen from North America, Atmos. Environ., 34, 2205–2230, 2000. 1479

Helmig, D., Pollock, W., Greenberg, J., and Zimmerman, P.: Gas chromatography mass spectrometry analysis of volatile organic trace gases at Mauna Loa Observatory, Hawaii, J. Geophys. Res., 101, 14 697–14 710, 1996. 1480
Hoshino, M., Akimoto, H., and Okuda, M.: Photochemical oxidation of benzene, toluene, and ethylbenzene initiated by OH radicals in the gas phase, Bull. Chem. Soc. Jpn., 51, 718–724, 1978. 1493, 1497
Houweling, S., Dentner, F., and Lelieveld, J.: The impact of nonmethane hydrocarbon compounds on tropospheric photochemistry, J. Geophys. Res., 103, 10 673–10 696, 1998. 1479
IPCC: Climate Change 2001: The Scientific Basis, Cambridge University Press, Cambridge, 2001. 1479
Katritzky, A. R., Ignatchenko, E. S., Barcock, R. A., Lobanov, V. S., and Karelson, M.: Prediction of gas chromatographic retention times and response factors using a general quantitative structure-property relationship treatment, Anal. Chem., 66, 1799–1807, 1994. 1483
Krivácsy, Z., Gelencser, A., Mészáros, G. E., Molnár, A., Hoffer, A., Mészáros, T., Sárvári, Z., Temesi, D., Varga, B., Baltensperger, U., Nyeki, S., and Weingartner, E.: Study on the chemical character of water soluble organic compounds in fine atmospheric aerosol at the Jungfraujoch, J. Atmos. Chem., 39, 235–259, 2001. 1479
Kwok, E. S. C. and Atkinson, R.: Estimation of hydroxyl radical reaction rate constants for gas-phase organic compounds using a structure-reactivity relationship: an update, Atmos. Environ., 29, 1685–1695, 1995. 1496
Lelieveld, J., Berresheim, H., Borrmann, S., Crutzen, P. J., Dentener, F. J., Fischer, H., Feichter, J., Flatau, P., Heland, J., Holzinger, R., Kormann, R., Lawrence, M. B., Levin, Z., Markowicz, K., Mihalopoulos, N., Minikin, A., Ramanthan, V., de Reus, M., Roelofs, G. J., Scheeren, H. A., Sciare, J., Schlager, H., Schulz, M., Siegmund, P., Steil, B., Stephanou, E. G., Stier, P., Traub, M., Warneke, C., Williams, J., and Ziereis, H.: Global air pollution crossroads over the Mediterranean, Science, 298, 794–799, 2002. 1479, 1480
Lewis, A. C., Carslaw, N., Marriott, P. J., Kinghorn, R. M., Morrison, P., Lee, A. L., Bartle, K. D., and Pilling, M. J.: A larger pool of ozone-forming carbon compounds in urban atmospheres, Nature, 405, 778–781, 2000. 1480
Limbeck, A. and Puxbaum, H.: Organic acids in continental background aerosols, Atmos. Environ., 33, 1847–1852, 1999. 1479
McKeen, S. A. and Liu, S. C.: Hydrocarbon ratios and photochemical history of air masses, Geophys. Res. Lett., 20, 2363–2366, 1993. 1495

Mihalopoulos, N., Stephanou, E., Kanakidou, M., Pilitsidis, S., and Bousquet, P.: Tropospheric aerosol ion composition in the Eastern Mediterranean region, Tellus, 49B, 314–326, 1997. 1481, 1489

Nolting, F., Behnke, W., and Zetzsch, C.: A smog chamber for studies of the reactions of terpenes and alkanes with ozone and OH, J. Atmos. Chem., 6, 47–59, 1988. 1491, 1506

O'Dowd, C., Aalto, D. P., Hämeri, K., Kulmala, M., and Hoffmann, T.: Atmospheric particles from organic vapours, Nature, 416, 497, 2002. 1479

Ohta, T. and Ohyama, T.: A set of rate constants for the reactions of OH radicals with aromatic hydrocarbons, Bull. Chem. Soc. Jpn., 58, 3029–3030, 1985. 1491, 1506

Rappenglück, B., Fabian, P., Kalabokas, P., Viras, L. G., and Ziomas, I. C.: Quasi-continuous measurements of non-methane hydrocarbons (NMHC) in the Greater Athens Area during MEDCAPHOT-TRACE, Atmos. Environ., 32, 2103–2121, 1998. 1480, 1484, 1506

Roberts, J. M., Fehsenfeld, F. C., Liu, S. C., Bollinger, M. J., Hahn, C., Albritton, D. L., and Sievers, R. E.: Measurements of aromatic hydrocarbon ratios and NO_x concentrations in the rural troposphere: Observation of air mass photochemical aging and NO_x removal, Atmos. Environ., 18, 2421–2432, 1984. 1495, 1497

Roberts, J. M., Bertman, S. B., Parrish, D. D., and Fehsenfeld, F. C.: Measurement of alkyl nitrates at Chebogue Point, Nova Scotia, during the 1993 North Atlantic Regional Experiment (NARE) intensive, J. Geophys. Res., 103, 13 569–13 580, 1998. 1492, 1493, 1495

Roberts, J. M., Stroud, C. A., Jobson, B. T., Trainer, M., Hereid, D., Williams, E., Fehsenfeld, F., Brune, W., Martinez, M., and Harder, H.: Application of a sequential reaction model to PANs and aldehyde measurements in two urban areas, Geophys. Res. Lett., 28, 4583–4586, 2001. 1492, 1493, 1495

Rudolph, J. and Johnen, F. J.: Measurements of light atmospheric hydrocarbons over the Atlantic in regions of low biological activity, J. Geophys. Res., 95, 20 583–20 591, 1990. 1495, 1497

Salisbury, G., Williams, J., Holzinger, R., Gros, V., Mihalopoulos, N., Vrekoussis, M., Sarda-Estéve, R., Berresheim, H., von Kuhlmannand, R., Lawrence, M., and Lelieveld, J.: Ground-based PTR-MS measurements of reactive organic compounds during the MINOS campaign in Crete, July–August 2001, Atmos. Chem. Phys. Discuss., 3, 911–948, 2003. 1482, 1485, 1486, 1490, 1497, 1498, 1507

Stroud, C. A., Roberts, J. M., Goldan, P. D., Kuster, W. C., Murphy, P. C., Williams, E. J., Hereid, D., Parrish, D., Sueper, D., Trainer, M., Fehsenfeld, F. C., Apel, E. C., Riemer, D., Wert, B.,

Henry, B., Fried, A., Martinez-Harder, M., Harder, H., Brune, W. H., Li, G., Xie, H., and Young, V. L.: Isoprene and its oxidation products, methacrolein and methylvinyl ketone, at an urban forested site during the 1999 Southern Oxidants Study, J. Geophys. Res., 106(D8), 8035–8046, 2001. 1492, 1495, 1498

Wang, Y., Jacob, D. J., and Logan, J. A.: Global simulation of tropospheric O_3-NO_x-hydrocarbon chemistry, 3. Origin of tropospheric ozone and effects of nonmethane hydrocarbons, J. Geophys. Res., 103, 10 757–10 767, 1998. 1479

Wedel, A., Müller, K.-P., Ratte, M., and Rudolph, J.: Measurements of volatile organic compounds (VOC) during POPCORN 1994: Applying a new on-line GC-MS-Technique, J. Atmos. Chem., 31, 73–103, 1998. 1480

Xu, X., van Stee, L. L. P., Williams, J., Beens, J., Adahchour, M., Vreuls, R. J. J., Brinkman, U. A. Th., and Lelieveld, J.: Comprehensive two-dimensional gas chromatography (GC×GC) measurements of volatile organic compounds in the atmosphere, Atmos. Chem. Phys. Discuss., 3, 1139–1181, 2003. 1480, 1481, 1483

Table 1. Statistics of atmospheric hydrocarbons observed at Finokalia, Crete during the MINOS campaign, and mean hydrocarbon mixing ratios in the Greater Athens Area, Greece

Compound	Mean±1σ (pptv)	n	LOD$_i$[a] (pptv)	LOD$_{ii}$[b] (pptv)	GAA Mean[c] (ppbv)	Estimated Age[d] (h)
Octane	11±7	82	3	4	0.1	16
Nonane	8±6	86	5	3	0.2	20
Decane	11±6	87	12	8	0.2	16
Undecane	8±5[e]	87	19	12	0.1	11
Toluene	43±36	86	15	5	6.7	48
Ethylbenzene	7±4	87	9	2	1.3	43
p-/m-Xylene[f]	12±7	88	17	4	3.2	
o-Xylene	25±18	88	21	5	1.5	19
Propylbenzene	6±4	88	6	1	1.4[h]	59
i-Propylbenzene	1±1[e]	72	2	2		
1,2,3-Trimethylbenzene	3±2	76	5	1		
1,3,5-Trimethylbenzene	5±6	84	3	1	0.3	4
1-Methyl-2-ethylbenzene	6±9	78	6	3	1.8[i]	27
1-Methyl-3/4-ethylbenzene[g]	10±12	86	35	0.3	0.7	
Indane	1±1[e]	62	3	3		
1,3-Diethylbenzene	2±1[e]	72	5	2		
1,4-Diethylbenzene	2±3[e]	83	2	1		
Acetophenone	94±53	91	11	11		
Benzeneacetaldehyde	3.6±2.6	86	0.2	0.2		

ACPD
3, 1477–1513, 2003

Table 1. Continued

[a] For the period 2–12 August 2001.
[b] For the period 13–21 August 2001.
[c] From the measurements at a suburban site in Athens during the period 20 August–20 September 1994 (Rappenglück et al., 1998). The measurements were made on an on-line GC-FID system. The estimated overall accuracy and precision were 20% and 10–15%, respectively. The (3σ) detection limit was 0.01–0.08 ppbv.
[d] Photochemical ages estimated under the assumptions that the mean concentration profile obtained at Finokalia was a photochemically aged concentration profile of the GAA air and that the background levels were negligible for all the components. Reaction constants from literature (Atkinson, 1986; Atkinson and Aschmann, 1989; Nolting et al., 1988; Ohta and Ohyama, 1985) and the average OH concentration of 4.5×10^6 cm^{-3} for the MINOS campaign (Berresheim et al., 2003) were used for calculating the photochemical ages.
[e] Highly uncertain, under the detection limit for most of the time.
[f] p-xylene and m-xylene co-elution.
[g] 1-Methyl-3-ethylbenzene and 1-methyl-4-ethylbenzene co-elution.
[h] Co-elution with dodecane.
[i] Co-elution with styrene.

ACPD
3, 1477–1513, 2003

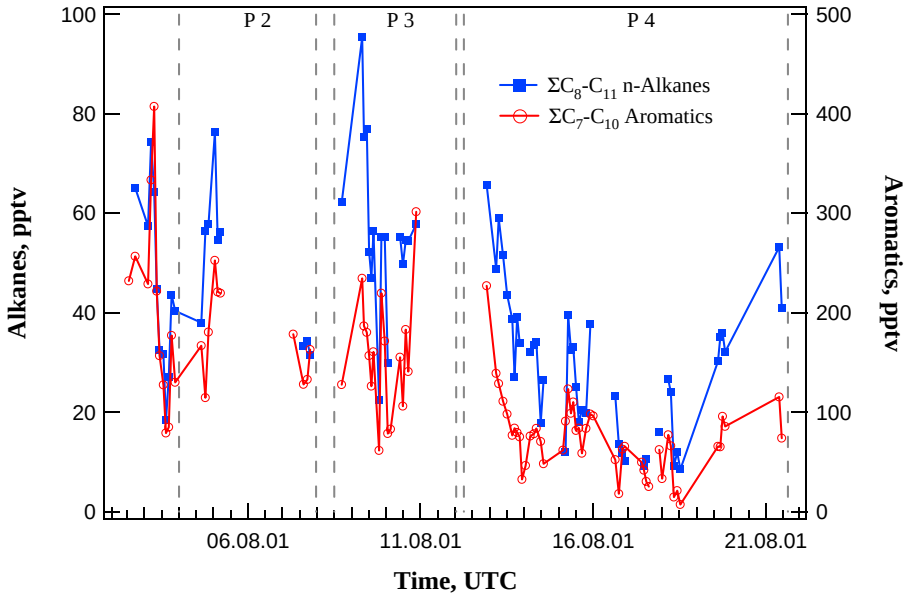

Fig. 1. Summed mixing ratios of C_8-C_{11} n-alkanes and C_7-C_{10} aromatics during the MINOS campaign. Due to interferences, 1,2,4-trimethylbenzene is not included in the mixing ratio of aromatics. The vertical dashed lines show the starts and ends of periods 2–4 (see Salisbury et al., 2003).

ACPD
3, 1477–1513, 2003

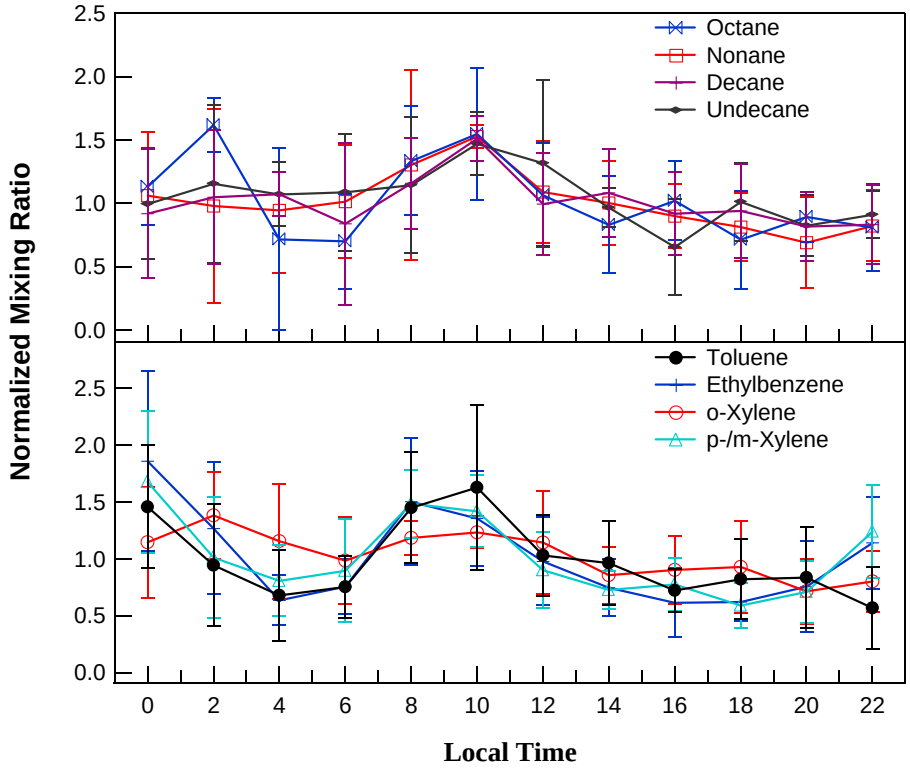

Fig. 2. Normalized and averaged diel profiles of selected hydrocarbons. The error bars represent one standard deviation.

ACPD
3, 1477–1513, 2003

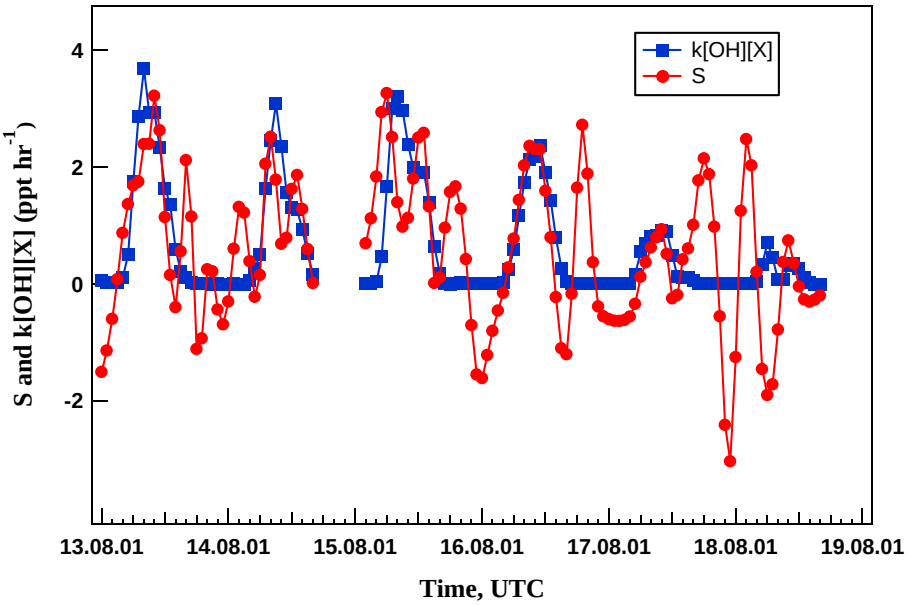

Fig. 3. Variations in the net physical source/sink (S) and chemical sink (k[OH][X]) of ethylbenzene during the period 13–19 August 2001.

ACPD
3, 1477–1513, 2003

GC×GC measurements of C_7 – C_{11} hydrocarbons

X. Xu et al.

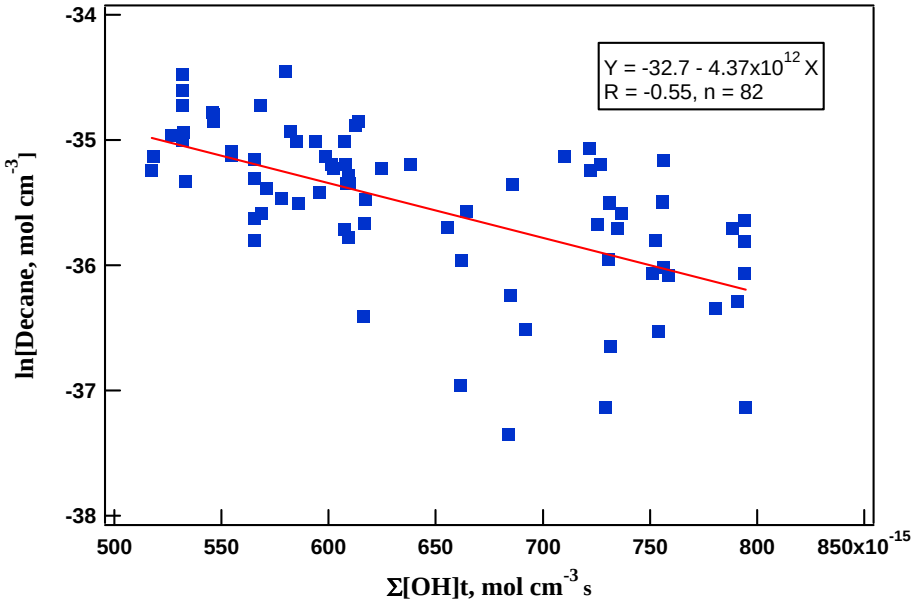

Fig. 4. Relationship between the mixing ratio of n-decane and the integral of OH abundance over a 24-h period prior to hydrocarbon measurement. Note that $/n$[Decane] is used instead of [Decane] and that the units are chosen so that the slope of the regression line can be compared with the OH rate constant k in $cm^3\ mol^{-1}\ s^{-1}$.

ACPD
3, 1477–1513, 2003

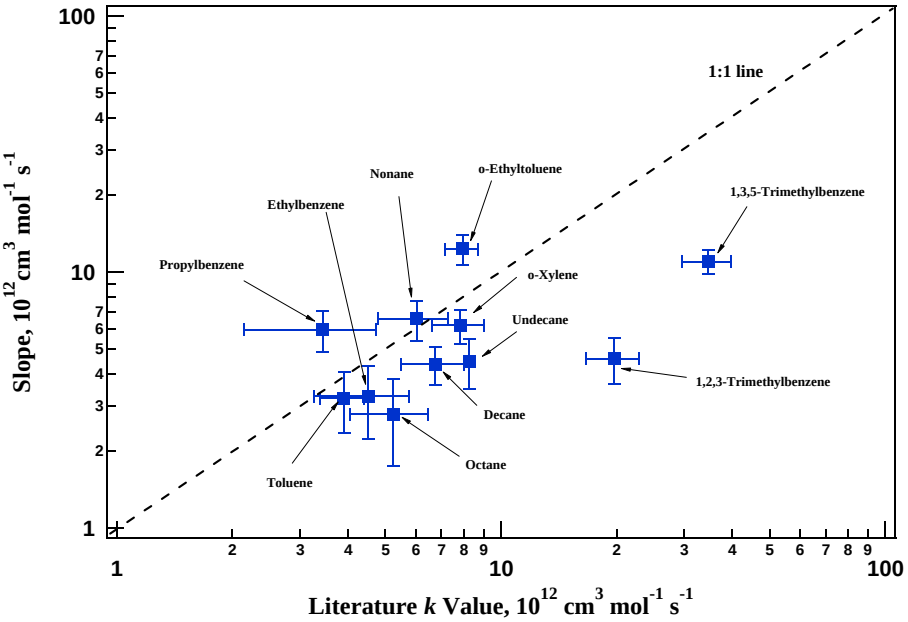

Fig. 5. Comparison of slopes of the $ln[X] - \sum[OH]t$ correlation lines for different components with literature k values. The horizontal bars represent the reported errors in the k values. The vertical bars are the standard deviations of the slopes.

ACPD
3, 1477–1513, 2003

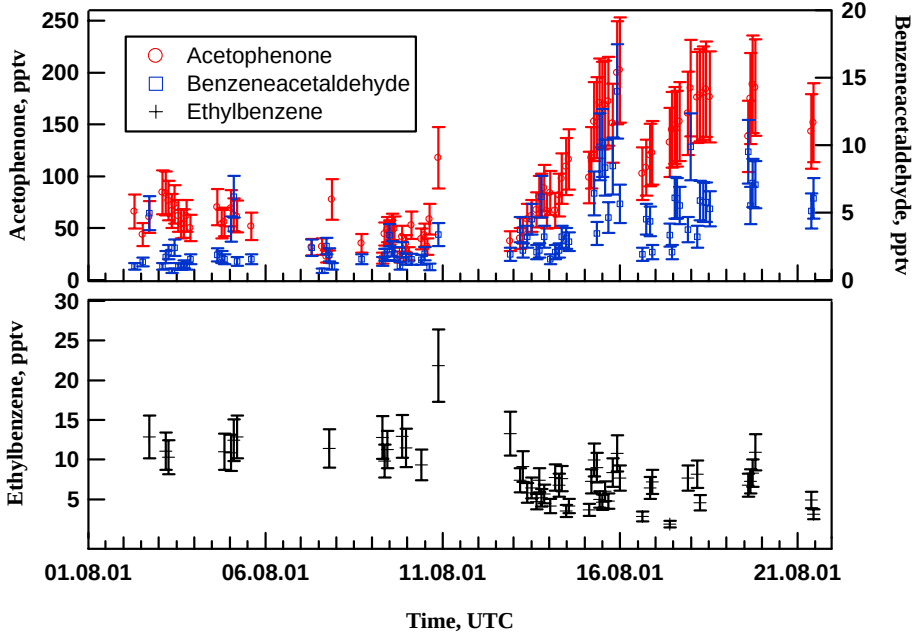

Fig. 6. Time series of ethylbenzene (bottom), acetophenone and benzeneacetaldehyde (top). The vertical bars represent the estimated errors.

ACPD
3, 1477–1513, 2003

GC×GC measurements of $C_7 - C_{11}$ hydrocarbons

X. Xu et al.

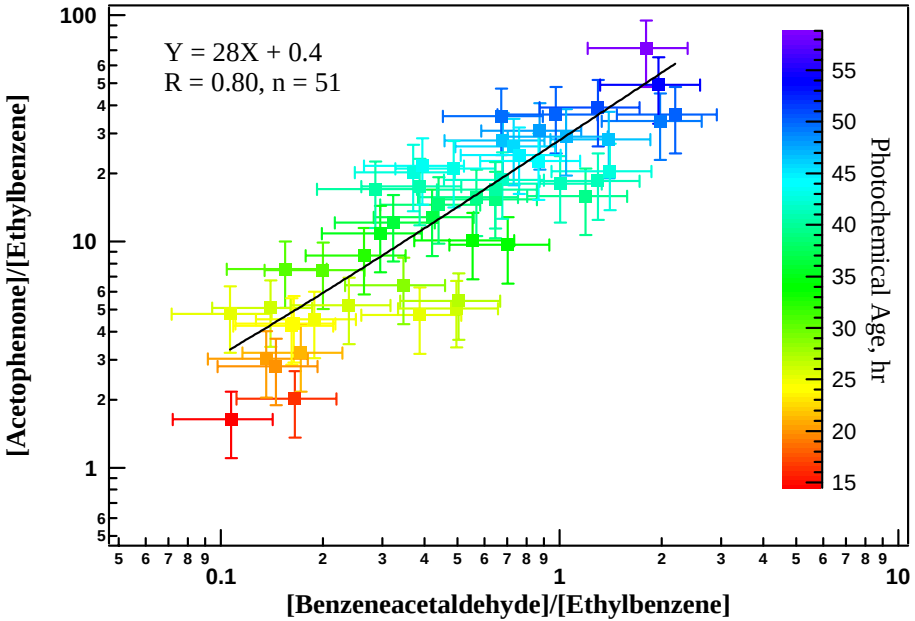

Fig. 7. Correlation between the ratios [acetophenone]/[ethylbenzene] and [benzeneacetaldehyde]/[ethylbenzene]. The vertical and horizontal bars represent the estimated errors in the ratios. Photochemical ages, as derived from the [acetophenone]/[ethylbenzene] ratios, are coded in color.

ACPD
3, 1477–1513, 2003